

Status of the crystallography beamlines at SSRF*

Jianhua He^a and Xingyu Gao

Shanghai Institute of Applied Physics, Chinese Academy of Sciences, Shanghai 201204, China

Received: 2 January 2014

Published online: 25 February 2015 – © Società Italiana di Fisica / Springer-Verlag 2015

Abstract. The Shanghai Synchrotron Radiation Facility (SSRF), an advanced intermediate-energy third-generation light source in China, was completed with seven phase-I beamlines opening to users in May 2009. Among these beamlines, there are two dedicated crystallography beamlines, one for macromolecular crystallography and one for crystallography in materials science, condensed matter physics and other relevant fields. The macromolecular crystallography beamline BL17U1, based on an in-vacuum undulator, has achieved very high brightness at the sample position with its flux of 4.1×10^{12} photons/s at 12 keV and focused beam size of FWHM ($H \times V$) $67 \times 23 \mu\text{m}^2$ in a small beam divergence over an energy range of 5–18 keV. Nowadays, there are about 200 user groups at this beamline with more than 330 structures solved each year. In the past, lots of significant results have been obtained at this beamline, such as the structural determination of important membrane proteins and proteins of viruses. In addition, three new macromolecular crystallography beamlines of different features have just been constructed and will soon open to users. To meet the rapidly growing user demands and the important scientific challenges, a few more dedicated crystallography beamlines have been proposed in the Phase-II Beamlines Project.

1 Introduction

The Shanghai Synchrotron Radiation Facility (SSRF) is an intermediate-energy third-generation light source built in Shanghai, China. The SSRF complex consists of a 150 MeV linac, a full energy booster, a 3.5 GeV storage ring of 432 m in circumference, and beamlines. The SSRF storage ring was designed to run at beam current up to 300 mA with a beam emittance of $3.9 \text{ nm} \cdot \text{rad}$ at 3.5 GeV. With advanced insertion devices, it can provide high-intensity X-rays of 10^{20} photons/(s · mm² · mrad² · 0.1% · BW) in the maximum brilliance. Seven beamlines were selected as phase-I beamlines aiming at the research fields of life science, physics and materials science, chemical science, environmental science, biomedicine, archeology and industrial applications. The construction of SSRF began on December 25, 2004 and was completed in April of 2009 with all the design performance achieved [1, 2].

SSRF opened to users in May of 2009 with seven phase-I beamlines in full operation. At the first stage, the storage ring was operated in beam decay mode with injections occurring two times per day at a twelve-hour interval. The typical operating beam current was from 210 mA to 140 mA with a beam lifetime of around 20 hours. Top-up operation for user experiments was commenced in December of 2012 [3], and the beam current was gradually increased from 210 mA to the present 240 mA. Each year it provides about 5500 hours of beamtime to beamlines, and among which at least 4500 hours are guaranteed for user experiments. All the beamlines receive regular user proposals twice a year, with the deadlines on 30th March and 30th September, respectively. In addition, long-term proposals for a two-year period were based on a peer-review process and received once a year with the deadline on 30th June. Proposals are requested to be submitted online through the web page <http://ssrf.sinap.ac.cn/proposals/>. In the past five years, about 5200 proposals were accepted, with an average success rate of 70%, but with a drastically reduced beamtime allocated for each proposal. The total beam time requested by the users is about 3 times of the operation hours available for experiments.

* Contribution to the Focus Point on “Status of third-generation synchrotron crystallography beamlines: An overview” edited by Gaston Garcia.

^a e-mail: hejh@sinap.ac.cn

Table 1. The dedicated crystallography beamlines in operation at SSRF.

Beamline	Scientific case	Experimental method	Supporting labs
Macromolecular crystallography (BL17U1)	Structural determination of protein crystals	Single crystal diffraction with tunable X-ray energy	Protein expression, purification and crystallization
X-ray diffraction (BL14B1)	Structural information of various materials, including polycrystalline powder, film and nano-materials.	Powder diffraction, X-ray reflectivity, grazing incidence X-ray diffraction	Basic sample preparation

2 Beamlines dedicated to crystallography at SSRF

Among the SSRF phase-I beamlines, there are two beamlines dedicated to crystallography, one is the macromolecular crystallography (MX) beamline named BL17U1, and the other is the X-ray diffraction beamline named BL14B1 for the structural studies of materials. (See table 1.)

BL17U1 is the first MX Beamline at the advanced synchrotron light source in China. It was aimed to meet various demands on structural determination as much as possible, from small crystals of $20\ \mu\text{m}$ size to the crystals of large unit cells up to $1000\ \text{\AA}$ dimension. The beamline was designed to have high flux beam with small beam divergence and reasonably small beam size, and it has achieved its design goals with a flux of 4.1×10^{12} photons/s and a focused beam size of FWHM ($H \times V$) $67 \times 23\ \mu\text{m}^2$ in a beam divergence of FWHM ($H \times V$) $0.3 \times 0.1\ \text{mrad}^2$. These features laid a solid base for the productivity of this beamline.

BL14B1 is a general purpose X-ray diffraction beamline. It is based on a bending magnet source and has employed a beamline optical setup mainly consisting of a collimating mirror, a sagittal focusing double-crystal monochromator and a vertical focusing mirror to facilitate both focusing and non-focusing working modes. It covers an energy range from 4 to 22 keV and achieves a photon flux of 10^{11} phs/s. A spot size of $0.4 \times 0.4\ \text{mm}^2$ can be obtained with a beam divergence of $2.5 \times 0.2\ \text{mrad}^2$ ($H \times V$) in the focusing mode whereas a $0.02\ \text{mrad}$ vertical divergence can be obtained in the non-focusing mode.

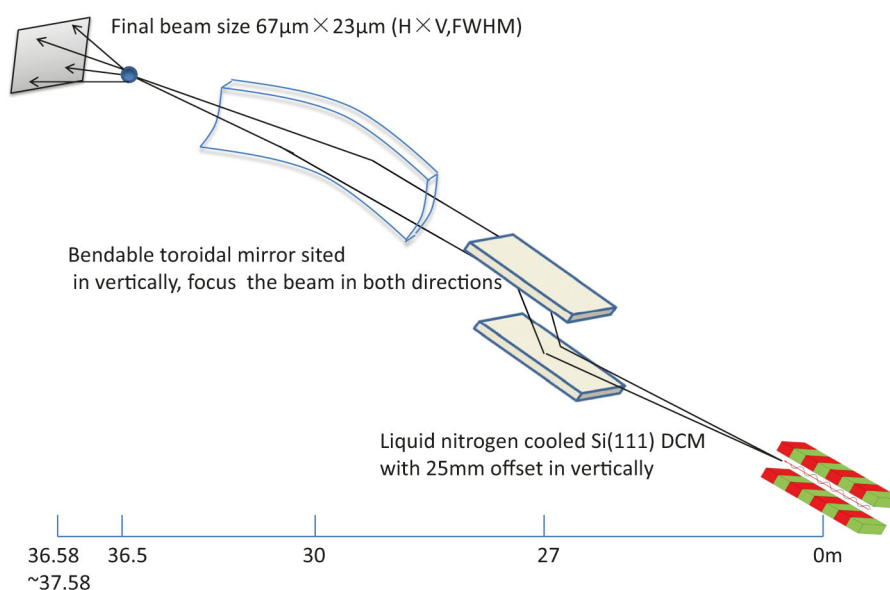
The number of SSRF users kept increasing with time, partly due to the stimulation of SSRF operation itself. The macromolecular crystallography beamline witnessed a very rapid expansion of its user community, from less than 50 user groups initially in 2009 to about 200 user groups at present. One dedicated MX beamline is definitely not enough to meet users' demands. In order to address this issue, the construction of three new MX beamlines started in December of 2010, as a part of the so-called National Facility for Protein Science project. These three beamlines were designed to have different features to meet various requirements of user experiments. Among these beamlines, one specializes in protein micro-crystallography with a minimum focused beam size of around 5 microns, and another one is for the structural determination of large complexes with a very parallel beam. The third one is for high-throughput screening and data collection of standard crystals. All these three beamlines are in final commissioning and will soon be open to users.

Besides the above beamlines in operation and in commissioning, there are another three dedicated crystallography beamlines proposed within the project of SSRF Phase-II Beamlines to meet more specific scientific challenges. One beamline is aimed to cope with the difficult membrane protein structures by using one-micron and even sub-micron X-ray beam, and one will be equipped with bio-safety protection capability BSL2 (*i.e.* P2 in China) for the structural studies of protein crystals of live viruses. The third crystallography beamline makes use of Laue microdiffraction in order to facilitate the studies of local microstructures of heterogeneous materials and microcrystal structures as well as their evolution dynamics. Table 2 is a brief summary of all these crystallography beamlines in commissioning and in planning.

Currently, there is a dedicated laboratory to support the users at the MX Beamline BL17U1 for protein expression, purification and crystallization. Meanwhile, basic sample preparation conditions are also provided in a lab close to X-ray Diffraction Beamline BL14B1 including sample heat treatments in furnaces. In the SSRF Phase-II project, plan has been made to build additional ancillary laboratories to provide various equipments for sample preparation and necessary standard characterization of different samples, which surely will benefit all the users at crystallography beamlines.

Table 2. New crystallography beamlines in commissioning/planning at SSRF.

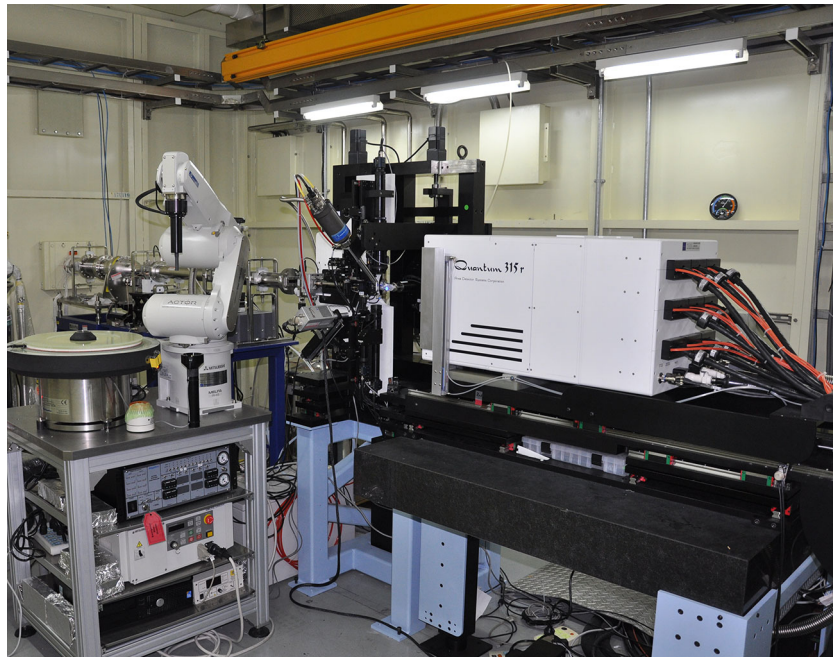
Beamline	Source	Energy range (keV)	Status
Protein micro-crystallography BL18U1	U25	5–18	In commissioning
Protein complex crystallography BL19U1	U20	7–15	In commissioning
High-throughput protein crystallography BL17B1	BM	5–20	In commissioning
Membrane protein	U	7–20	In planning
P2 protein crystallography	U	7–18	In planning
Laue microdiffraction	BM	7–30	In planning

**Fig. 1.** Schematic layout of the beamline optical setup.

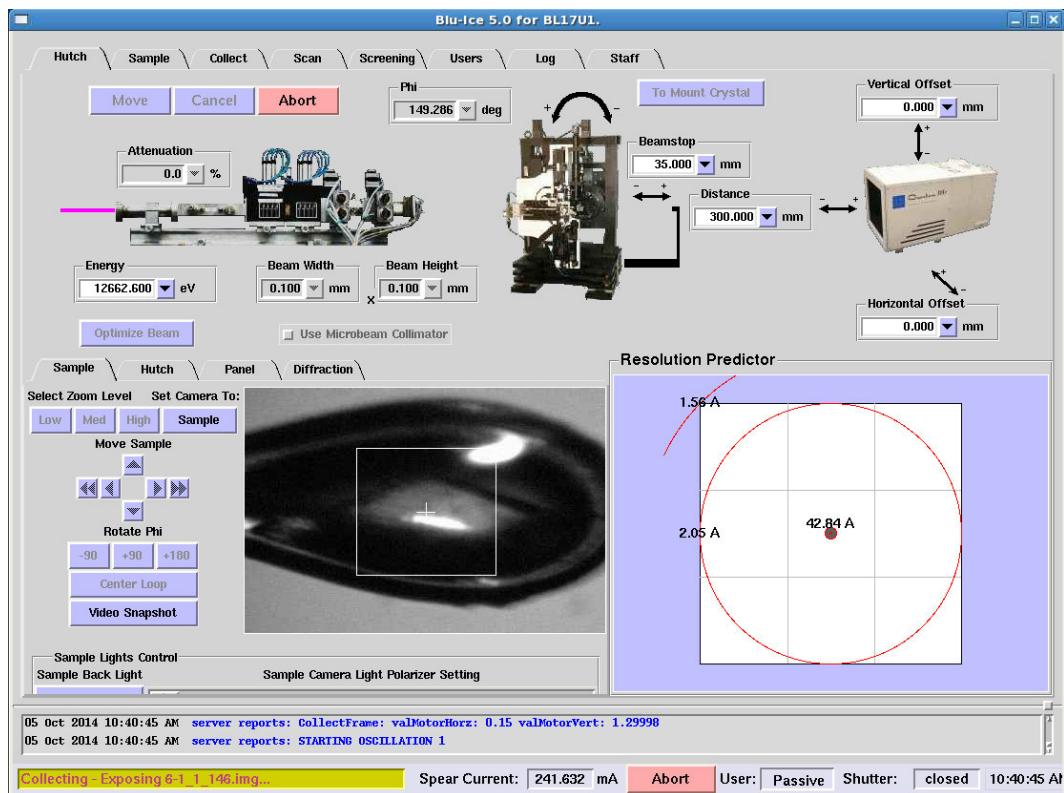
3 Example of a crystallography beamline: BL17U1

The beamline BL17U1 employed an in-vacuum undulator as the source to achieve high brilliance. The undulator has a period length of 25 mm and has 80 magnetic periods with total length of 2 m and can work at a minimum gap of 6 mm. It can cover the energy range of 5 to 18 keV continuously by using 3rd to 9th harmonics. The major optical components include a liquid-nitrogen-cooled Si(111) double-crystal monochromator (DCM), bought from Accel company, and a bent toroidal mirror which reflects the beam horizontally and focuses the beam both horizontally and vertically. The mirror was made of silicon and coated with Rh, bought from SESO, and its meridional slope error is less than $2 \mu\text{rad}$ and its sagittal slope error is less than $15 \mu\text{rad}$. The horizontal focusing is achieved by a mirror bender from TOYAMA and the bending curvature of the mirror can be adjusted to focus the beam at the wanted position. The vertical focusing is achieved by the sagittal radius of the mirror and it can also be adjusted by changing the grazing angle slightly. The demagnification ratio of 5:1 was designed for the beamline in order to focus the beam to tens of microns. The schematic optical layout of the beamline is shown in fig. 1. The distance from the source to sample is 36.5 m.

The end station (fig. 2(a)) consists mainly of the beam-conditioning devices, a single-axis goniometer from Crystal Logic Inc., an automatic sample changer and a CCD detector. Diffraction data are collected using an ADSC Q315r CCD detector mounted on a three-axis support table, which is separated from the support stage of the goniometer. Both stages for the goniometer and the detector were bought from Crystal Logic and can be positioned in pitch, roll and yaw angles with 0.5 micron resolution. The distance between the sample and the detector can be set from 85 mm to 1000 mm. The sample changer robot, an ACTOR from Rigaku, has been used and it accepts the universal pucks holding up to 80 samples each time. The SOC of the air-bearing axis of the goniometer is $\pm 2 \mu\text{m}$ and the servo motor with encoder can assure a resolution of 0.0001 degree. The single-axis goniometer head can be replaced by a mini-kappa when necessary, but it does not work with the sample changer robot. And so it is not used in routine operation and was rarely used in practice.



(a)



(b)

Fig. 2. View of the end station (a) and the Blu-Ice GUI (b).

Table 3. Summary of the beamline BL17U1 parameters.

Beamline name	BL17U1
Source type	In-vacuum undulator, 25 mm \times 80 periods
Monochromator	Cryo-cooled double flat crystal Si(111)
Energy range	5–18 keV
Energy resolution	$< 2.0 \times 10^{-4}$
Flux (at 12 keV 20 mA) ^(a)	4.1×10^{12} phs/s
Focused beam size (FWHM) ^(a)	$67 \mu\text{m} \times 23 \mu\text{m}$, H \times V
Beam divergence	$0.3 \text{ mrad} \times 0.1 \text{ mrad}$
Goniometer	Single-axis, Crystal Logic
Cryo capability	100 K
Sample mounting	Manually/Rigaku ACTOR robot
Detector model	CCD, Q315r
2Theta capability	None

^(a) The flux at different energies from 7 to 18 keV is all measured by a calibrated ionization chamber with the maximum flux of 4.2×10^{12} phs/s at 13 keV and the minimum flux of 9×10^{11} phs/s at 7 keV, and the beam size at sample position was measured by the knife-edge scan.

The sample environment is cooled down to 100 K by using a liquid-nitrogen cooler, Oxford Cryostream 700. There are two sets of cameras visualizing the sample. One is from the top of the sample with high magnification, and the other is an on-axis camera with fixed low or medium magnification. A Hitachi vortex Si-drift detector can be moved pneumatically close to the sample for MAD scans and X-ray excitation experiments. A self-designed attenuator consisting of 12 aluminum foils is installed to change the beam flux on the sample and users can simply select the percentage of attenuation they want from a list provided. The beam intensity can be monitored by a small ion chamber in the goniometer arm and an active beamstop [4] after the sample. The beam position is monitored by a QBPM from Oxford FBM and the 24 hour drift is less than $5 \mu\text{m}$ in both directions. The beamline specifications and main parameters are summarized in table 3.

Friendly graphic user interface (GUI) (fig. 2(b)) has been developed for user experiments based on the open source software Blu-Ice [5] and EPICS [6] control system. Useful functions for experiments have been integrated into GUI with continued efforts [7], including automatic beam optimization, the synchronization of the energy and the undulator gap during energy scan and the sample mounting by robot, etc. The functional system with intuitive GUI ensures that the beamline is easy to use and reliable. Now users can have remote access to the beamline carrying out remote data collection through virtual private network (VPN) connection.

At this beamline, 20 crystals can be screened for diffraction quality in one hour. About 4.7 datasets (180 1-degree frames with 1 second exposure/frame) can be collected in an hour. 200 ms exposure is the limit to obtain high-quality dataset according to our test, although the fast shutter from Crystal Logic Inc. itself supports up to 100 ms exposure. For the experiments requesting a smaller beam size, users can easily select a pinhole, made of platinum-iridium alloy, with size of 50, 20, 10 or $5 \mu\text{m}$. An aperture of $300 \mu\text{m}$ is always used to reduce the scattering.

Users can change the energy easily by themselves. An energy change from 13 keV to 7 keV takes about 90 seconds including beam auto-optimization. A small energy change of 500 eV takes about 10 seconds and it is not necessarily to re-optimize the beam in this case. The MAD experiments are run automatically, and wedged anomalous data collection is available. At present, we are implementing automated loop-centering software and the webice system originated from SSRL [8], which can handle large numbers of samples semi-automatically.

Users have access to the ancillary laboratory for preparing samples near the beamline. The lab provides conditions for users to prepare protein crystal samples on site. Conventional instruments have been equipped in the laboratory, including incubator shakers, centrifuges, an AKTA purifier, an ultraviolet spectrophotometer, a nanoparticle size analyzer, a nanoliter high-throughput liquid handing system, and stereomicroscopes. During the user experiment, 24 hour on-site user support is provided by an on-duty staff in order to solve the problem promptly, and the extra support can be called on whenever it is needed.

4 Examples of science at crystallography beamlines

As the first dedicated macromolecular crystallography beamline at SSRF, BL17U1 has a big number of user groups and a lot of important protein structures, including membrane proteins, protein complexes and virus-related proteins, have been solved using this beamline. During the past two years, more than 330 structures were deposited to the

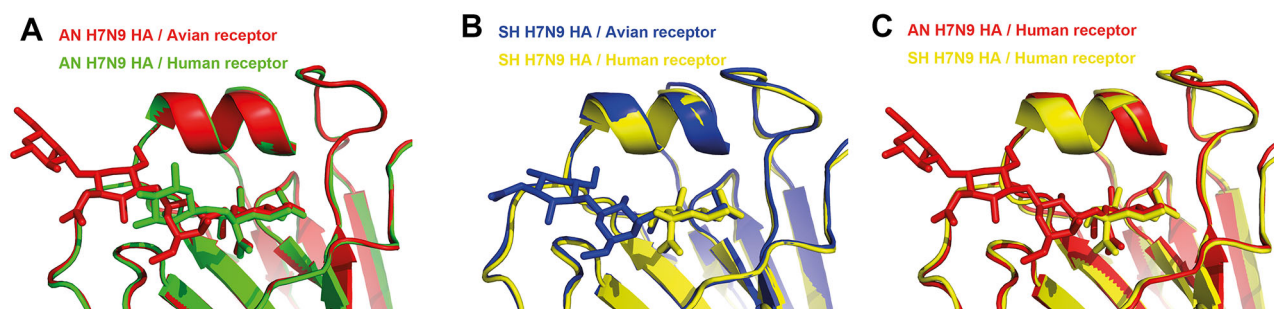


Fig. 3. Structural comparison of AH-H7N9 HA and SH-H7N9 HA complexes. Human and avian receptor analogs are α -2, 6-linked galactose and α -2, 3-linked galactose, respectively. The figure was generated by using PyMOL.

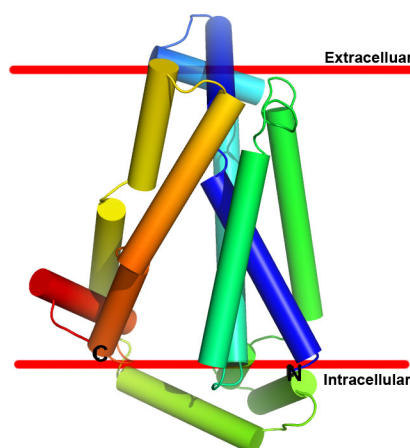


Fig. 4. The crystal structure of human GLUT1. N-terminal and C-terminal of protein were drawn in blue and orange, respectively.

Protein Data Bank (PDB) every year and total structures deposited in PDB surpass 1000 in less than five years, among which 18% are determined by SAD or MAD. Besides the academic users, 14 pharmaceutical companies have used this beamline by contract. The following are two examples of research work done at the beamline.

Highly pathogenic avian influenza tracing and trans-species transmission mechanism research serve as the basis for scientific judgment and scientific prevention and control of flu. In the human infection of H7N9 avian influenza breaking out at the end of February 2013 in China, the virus involved was a kind of new recombinant virus. Gao's group focused on two viral strains firstly reported in this influenza outbreak, *i.e.* AH-H7N9 from Anhui of China and SH-H7N9 from Shanghai of China. By using BL17U1 timely without any delay, they soon analyzed the hemagglutinin proteins of the two viral strains and their mutants as well as the complex structures of human and avian receptor analogs (see fig. 3). The resolution ranges of structures are from 2.6 to 3.1 angstrom. These results expound the structural basis of the change of receptor binding ability. The detailed interpretation of the H7N9 virus from viral source tracing, trans-host transmission, epidemiology and immunology as well as clinical medicine, provides an important theoretical basis for prevention and control strategies against the recurrence and the outbreak of new type influenza of the H7N9 virus [9]. The structures had been deposited to the Protein Data Bank, and PDB IDs are 4KOL, 4KOM, 4KON, 4LCX, 4LKG, 4LKH, 4LKI, 4LKJ, and 4LKK.

GLUT1 is a membrane protein that is responsible for the uptake of glucose into erythrocytes and other cells. Yan's group had reported the structure of a proton-coupled xylose symporter that is a bacterial homologue of GLUT1 in 2012 [10]. Two years later, they determined the structure of human GLUT1 in an inward-open conformation finally and the resolution is 3.2 angstrom (fig. 4). After analyzing the structure of the human protein, it clearly interpreted inactivating mutations associated with GLUT1 deficiency syndrome, which is referred to as the De Vivo syndrome [11]. Glucose surge in demand for cancer cell, and elevated expression levels of GLUT1 have been observed in several cancer types, so GLUT1 is also a potential drug target. This structure was deposited to Protein Data Bank, and the PDB ID is 4PYP.

Meanwhile, a lot of crystallography experiments of various materials including powder and thin films have also been carried out at X-ray diffraction beamline BL14B1. Here is an example of structural studies of hydrogen storage material Ammonia borane, one of the most promising hydrogen storage materials. Chen *et al.* determined the crystal structure of the light metal (Li) doped Ammonia borane, which expands the research field of B-N related chemicals and provides theoretical basis and technical support for new hydrogen storage materials [12].

5 Conclusions

Two crystallography beamlines at SSRF have been in operation for five years with users increasing rapidly, especially for the macromolecular crystallography beamline. Big effort has been made to expand the capability of protein structure determination at SSRF with three new beamlines constructed recently. A few more crystallography beamlines have been planned in SSRF phase-II beamlines project, including two dedicated protein crystallography beamlines with specific features for membrane proteins and live virus and one for microstructures of materials by using Laue micro-diffraction. Also in this project the capability of related ancillary laboratories for crystallography experiments will be greatly improved with systematic sample preparation and comprehensive off-line analysis tools. It is expected that SSRF phase-II beamlines will be completed before 2020, which will inevitably promote science at SSRF to a new stage.

Crystallography beamlines at SSRF have been designed and constructed by the SSRF Macromolecular Crystallography Beamline Group and Diffraction Beamline Group, together with SSRF Beamline Engineering Division. We thank all those colleagues for their contributions. We would also like to thank our users, Prof. G.F. Gao, N. Yan and P. Chen for contributing excellent examples of science cited in this paper.

References

1. M.H. Jiang, X. Yang, H.J. Xu, Z.T. Zhao, H. Ding, *Chin. Sci. Bull.* **54**, 4171 (2009).
2. David Cyranoski, *Nature* **459**, 16 (2009).
3. Z.T. Zhao, L.X. Yin, Y.B. Leng, W.Z. Zhang, B.C. Jiang, S.Q. Tian, *Performance optimization and upgrade of the SSRF storage ring*, in *Proceedings of IPAC13, Shanghai, China* (2013) pp. 178-180.
4. Q.Y. Pan, Q.S. Wang, Z.J. Wang, L. Li, J.H. He, *Nucl. Instrum. Methods Phys. Res. A* **735**, 584 (2014).
5. T.M. McPhillips, S.E. McPhillips, H.J. Chiu, A.E. Cohen, A.M. Deacon, P.J. Ellis, E. Garman, A. Gonzalez, N.K. Sauter, R.P. Phizackherley, S.M. Solits S M, P. Kuhn, *J. Synchrotron Radiat.* **9**, 401 (2002).
6. R.K. Martin, *EPICS Input/Output Controller(IOC) Application Developer's Guide*, Argonne National Laboratory (2007).
7. Q.S. Wang, S. Huang, B. Sun, L. Tang, J.H. He, *Nucl. Techn.* **35**, 5 (2012).
8. A. González, P. Moorhead, S.E. McPhillips, J. Song, K. Sharp, J.R. Taylor, P.D. Adams, N.K. Sauter, S.M. Soltis, *Appl. Crystallogr.* **41**, 176 (2007).
9. Y. Shi, W. Zhang, F. Wang, J.X. Qi, Y. Wu, H. Song, F. Gao, Y.H. Bi, Y.F. Zhang, Z. Fan, C.F. Qin, H.L. Sun, J.H. Liu, J. Haywood, W.J. Liu, W.M. Gong, D.Y. Wang, Y.L. Shu, Y. Wang, J.H. Yan, G.F. Gao, *Science* **342**, 243 (2013).
10. L.F. Sun, X. Zeng, C.Y. Yan, X.Y. Sun, X.Q. Gong, Y. Rao, N. Yan, *Nature* **490**, 361 (2012).
11. D. Deng, C. Xu, P.C. Sun, J.P. Wu, C.Y. Yan, M.X. Hu, N. Yan, *Nature* **510**, 121 (2014).
12. C.Z. Wu, G.T. Wu, Z.T. Xiong, X.W. Han, H.L. Chu, T. He, P. Chen, *Chem. Mater.* **22**, 3 (2010).